AIAA JOURNAL
Vol. 32, No. 1, January 1994

Improved Method for Calculating Strain Energy Release Rate Based on Beam Theory

C. T. Sun* and R. K. Pandey†
Purdue University, West Lafayette, Indiana 47907

The Timoshenko beam theory was used to model cracked beams and to calculate the total strain-energy release rate. The root rotations of the beam segments at the crack tip were estimated based on an approximate two-dimensional elasticity solution. By including the strain energy released due to the root rotations of the beams during crack extension, the strain-energy release rate obtained using beam theory agrees very well with the two-dimensional finite element solution. Numerical examples were given for various beam geometries and loading conditions. Comparisons with existing beam models were also given.

Introduction

THE behavior of a crack in two-dimensional linear elastic solids is a subject of great interest. One of the main tasks in such studies is the calculation of the stress intensity factor. Except for limited cases, the stress analysis requires the use of numerical methods such as the finite element method. Since the stress is singular at the crack tip, a very fine finite element mesh must be used to accurately extract the stress intensity from the near-tip stress or displacement field. Since introduced by Rice[1] in 1968, the J integral has been widely used to calculate the strain-energy release rate along an integration path that is far from the crack tip, thus avoiding the need for an accurate description of the near-tip stress field. Recently, a crack closure method based on the finite element method proposed by Rybicki and Kanninen[2] for calculating the strain-energy release has been shown to be computationally efficient.[3]

In many cracked structures such as composite laminates containing delamination, each cracked or uncracked part is basically a beam. Calculation of the strain-energy release rate using two-dimensional elasticity theory is very cumbersome. It is quite common to use beam theory to estimate the strain-energy release rate based on the compliance method.[4] That is, for linear elastic solids, the strain-energy release rate G is equal to the variation of the total strain energy U in the system

$$G = \frac{\partial U}{\partial a} \tag{1}$$

where a indicates the crack size. Such an approach was used by Pook[5] to derive strain-energy release rates for many cracked beamlike structures under various kinds of loadings based on simple beam theory. Recently, Williams[6] and Nilsson and Storakers[7] expressed the strain-energy release rate in terms of the resultant axial and shear forces and moments of the beam segments that meet at the crack tip. Yin and Wang[8] used the J-integral method to calculate strain-energy release rate in terms of resultant axial forces and moments. Independently, a similar expression for mode II was obtained by Farris and Doyle[9] using the J integral with an integration path near the crack tip.

When the cracked portions are connected together with the uncracked portion at the crack tip (see Fig. 1), the assumption of plane sections remaining plane and the compatibility condition are enforced. Denoting the rotations of the three beam segments at the joint (crack tip) by θ_1, θ_2, and θ_3, respectively, the aforementioned conditions at the joint require that $\theta_1 = \theta_2 = \theta_3$; i.e., the joint is rigid in rotation. In reality, the beam assumptions (either Bernoulli-Euler or Timoshenko beam) break down in the vicinity of the crack tip, and the end rotations of the beam segments at the joint are, in general, different, as shown in Fig. 2.

To account for the flexibility of the joint at the crack tip in a double-cantilever beam (DCB) of isotropic materials, Kanninen[10,11] used the Timoshenko beam model to represent each part of the split beam. For each beam, the uncracked portion is supported by an elastic foundation consisting of linear and rotational springs with the spring constants given by

$$k_e = \frac{Eb}{(h/2)} \tag{2}$$

and

$$k_r = \kappa G b\,(h/2) \tag{3}$$

respectively. In Eqs. (2) and (3), E is the Young modulus, G is the shear modulus, b is the width of the beam, h is the thickness of each beam segment, and κ is a shear correction factor. Williams[12] extended this approach to include orthotropic

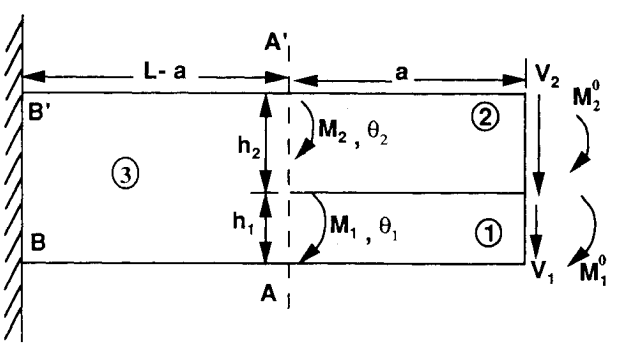

Fig. 1 Typical beam cracked lengthwise.

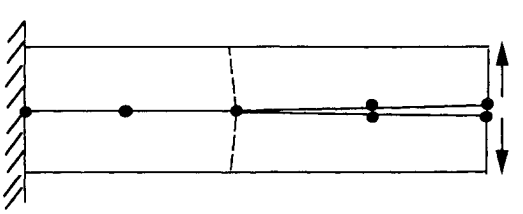

Fig. 2 Two-beam model allowing rotation at the crack tip.

Received April 16, 1993; revision received June 25, 1993; accepted for publication June 30, 1993.

*Professor, School of Aeronautics and Astronautics. Associate Fellow AIAA.

†Graduate Research Assistant, School of Aeronautics and Astronautics.

composite beams. It was shown that the correction of the joint flexibility can be made by replacing the original crack length a by an effective crack length $(a + \chi h)$ where χ is a coefficient that depends on the material constant and shear correction coefficient κ. For isotropic materials, Williams[12] found the error in the strain-energy release rate obtained using the beam on an elastic foundation model to be about 10% for $h/a = 0.1$. He suggested that the use of an empirical value $\kappa = 11/18$ (and, thus, $\chi = 0.66$) would yield a much improved solution.

Recently, Sankar and Hu[13] proposed a finite element formulation for a split composite beam to simulate dynamic delamination crack propagation in a composite laminate. As illustrated in Fig. 2, the beam is separated into upper and lower portions along the crack plane. The Timoshenko beam elements are formulated with nodes situated along the plane of the crack. Along the uncracked portion, three springs are introduced to connect the respective axial displacements, transverse displacements, and rotations of the upper and lower elements. Again, the major difficulty arises in choosing the proper values of these artificial spring constants, and it is often achieved by matching the beam solution with an "exact" two-dimensional finite element solution.

In this study, the root rotations of the beams meeting at the crack tip are evaluated by an approximate two-dimensional elasticity solution. The accuracy of the beam solutions for various beam geometries and loads is evaluated by comparison with two-dimensional finite element solutions.

Modeling Joint Flexibility

Consider the cracked beam of unit thickness loaded as shown in Fig. 1. The dimensions of the beam are characterized as L = length of the beam, a = crack length, h_1 = thickness of the lower beam part, and h_2 = thickness of the upper beam part; M_1 and M_2 are moments on the cross sections at the crack front due to the shear forces V_1 and V_2 and moments M_1^0 and M_2^0 on the beam parts 1 and 2, respectively, and θ_1 and θ_2 are the corresponding rotations of the two split beam parts at the crack front. For a relationship between the various M and θ, a half-plane plane-stress problem is posed as shown in Fig. 3. Planes AB and A′B′ correspond to the lower and upper surfaces of the beam, and plane AA′ indicates the cross section at the crack tip. It is assumed that the bending stresses on section AA′ are linearly distributed within each beam as indicated by the dashed lines in Fig. 3.

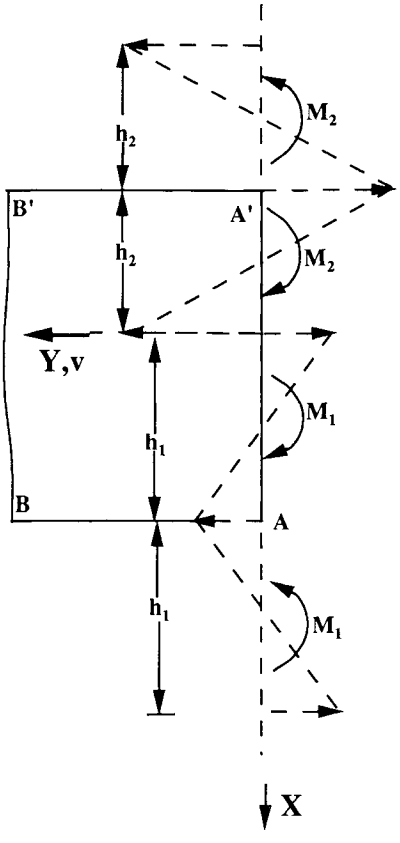

Fig. 3 Equivalent half-plane problem representing the beam model for obtaining the flexibility matrix at the crack tip of the joint.

If the half-plane subjected to these bending stresses applied on plane AA′ is analyzed, the traction-free condition on the upper beam surface (A′B′) and lower beam surface (AB) of the uncracked part is not satisfied. Since the root rotations of the upper and lower beams relative to the uncracked beam are significantly affected only by the shear traction on the AB and A′B′ surfaces, only the shear traction will be eliminated or minimized. This will be accomplished by adding an antimoment corresponding to each applied moment as shown in Fig. 3.

The displacement in the axial (y) direction in plane AA′ for an arbitrary normal stress $q(x)$ is given by Timoshenko and Goodier[14] as

$$v(x) = -\frac{2}{\pi E}\int_{-\infty}^{\infty} q(\zeta)\ell n\,|x-\zeta|\,d\zeta \tag{4}$$

where $-(2/\pi E)\ell n\,|x-\zeta|$ is the displacement solution for a unit concentrated force applied at $x = \zeta$.

For the moment loading shown in Fig. 3, the axial displacement on the AA′ plane is obtained as

$$\begin{aligned} v(x) = {} & -\frac{24M_1}{\pi E h_1^3}\left\{-\frac{h_1}{2}\left(x-\frac{h_1}{2}\right)+\frac{h_1^2}{8}\ell n\left|\frac{h_1-x}{x}\right|\right. \\ & \left.-\frac{[x-(h_1/2)]^2}{2}\ell n\left|\frac{h_1-x}{x}\right|\right\}+\frac{24M_1}{\pi E h_1^3}\left\{-\frac{h_1}{2}\left(x-\frac{3h_1}{2}\right)\right. \\ & \left.+\frac{h_1^2}{8}\ell n\left|\frac{2h_1-x}{h_1-x}\right|-\frac{[x-(3h_1/2)]^2}{2}\ell n\left|\frac{2h_1-x}{h_1-x}\right|\right\} \\ & -\frac{24M_2}{\pi E h_2^3}\left\{-\frac{h_2}{2}\left(x+\frac{h_2}{2}\right)+\frac{h_2^2}{8}\ell n\left|\frac{x}{h_2+x}\right|\right. \\ & \left.-\frac{[x+(h_2/2)]^2}{2}\ell n\left|\frac{x}{h_2+x}\right|\right\}+\frac{24M_2}{\pi E h_2^3}\left\{-\frac{h_2}{2}[x+(3h_2/2)]\right. \\ & \left.+\frac{h_2^2}{8}\ell n\left|\frac{h_2+x}{2h_2+x}\right|-\frac{[x+(3h_2/2)]^2}{2}\ell n\left|\frac{h_2+x}{2h_2+x}\right|\right\} \end{aligned} \tag{5}$$

Now, consider that the work done by the bending stresses in the regions 1 (h_1) and 2 (h_2) individually and require them to be equal to the work done by the respective moments (i.e., work equivalence):

$$M_1\theta_1 = -\int_0^{h_1}\sigma_1 v(x)\,dx \tag{6}$$

$$M_2\theta_2 = -\int_{-h_2}^{0}\sigma_2 v(x)\,dx \tag{7}$$

where

$$\sigma_1(x) = -\frac{12M_1}{h_1^3}\left(x-\frac{h_1}{2}\right) \qquad 0 \le x \le h_1 \tag{8}$$

$$\sigma_2(x) = -\frac{12M_2}{h_2^3}\left(x+\frac{h_2}{2}\right) \qquad -h_2 \le x \le 0 \tag{9}$$

Substituting Eq. (5) into Eqs. (6) and (7) and carrying the integrations, we obtain

$$\begin{Bmatrix}\theta_1\\ \theta_2\end{Bmatrix} = \begin{bmatrix}S_{11} & S_{12}\\ S_{21} & S_{22}\end{bmatrix}\begin{Bmatrix}M_1\\ M_2\end{Bmatrix} \tag{10}$$

where

$$S_{11} = \frac{48\ell n(2) - 12}{\pi E h_1^2}, \qquad S_{22} = \frac{48\ell n(2) - 12}{\pi E h_2^2}$$

$$S_{12} = \frac{24h_2}{\pi E h_1^3}\ell n\frac{h_1+h_2}{h_2} + \frac{12}{\pi E h_2^3 h_1^2}(h_1-h_2)(h_1+2h_2)^2\ell n\frac{h_1+2h_2}{h_1+h_2} - \frac{12(h_2+h_1)}{\pi E h_2^3}\ell n\frac{h_1+h_2}{h_1} + \frac{1}{\pi E h_1^2}(48\ell n 2 - 24) - \frac{12}{\pi E h_1 h_2} \quad (11)$$

$$S_{21} = \frac{24h_1}{\pi E h_2^3}\ell n\frac{h_2+h_1}{h_1} + \frac{12}{\pi E h_1^3 h_2^2}(h_2-h_1)(h_2+2h_1)^2\ell n\frac{h_2+2h_1}{h_2+h_1} - \frac{12(h_2+h_1)}{\pi E h_1^3}\ell n\frac{h_2+h_1}{h_2} + \frac{1}{\pi E h_2^2}(48\ell n 2 - 24) - \frac{12}{\pi E h_1 h_2}$$

In general, the rotation θ_3 of the uncracked beam at the crack tip is not zero. To obtain relative rotations (θ_1' and θ_2') of the upper and lower beams with respect to the uncracked portion, one must evaluate the rotation θ_3 of the uncracked beam. The relationship between θ_3 and $M_3 = M_1 + M_2$ is obtained by introducing antimoments M_3 on plane AA′ both above and below the beam surfaces so as to minimize the shear tractions at the upper and lower beam surfaces AB and A′B′ and then by applying the work-equivalence principle. This relation is obtained as

$$\theta_3 = S_0(M_1 + M_2) \quad (12)$$

where

$$S_0 = \frac{96\ell n(2) - 42}{\pi E(h_1 + h_2)^2} \quad (13)$$

A relationship between the relative rotations θ_1' and θ_2' and the local moments M_1 and M_2 is obtained by subtracting Eq. (12) from Eq. (10), and we obtain

$$\begin{Bmatrix}\theta_1' = \theta_1 - \theta_3\\ \theta_2' = \theta_2 - \theta_3\end{Bmatrix} = \begin{bmatrix}S_{11} - S_0 & S_{12} - S_0\\ S_{21} - S_0 & S_{22} - S_0\end{bmatrix}\begin{Bmatrix}M_1\\ M_2\end{Bmatrix} \quad (14)$$

The element of the $S - S_0$ matrix characterizes the compliances of the upper and lower beams at the joint (crack tip).

At this point, the shear stress free condition on planes AB and A′B′ is examined numerically. The shear stresses on these planes are obtained from a superposition of the half-plane elasticity solutions for linearly distributed loading stress $q(x)$ given by Timoshenko and Goodier.[14] The beam dimensions are $h_1 = 1$ cm and $h_2 = 4$ cm, and the loading is $M_1 = 1$ N-cm and $M_2 = -1$ N-cm. The material constants are $E = 70$ GPa and $\nu = 0.3$. Figures 4 and 5 show the shear stress distributions

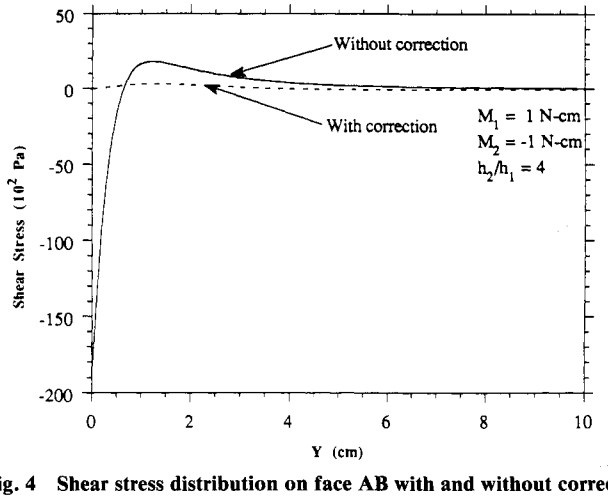

Fig. 4 Shear stress distribution on face AB with and without correction.

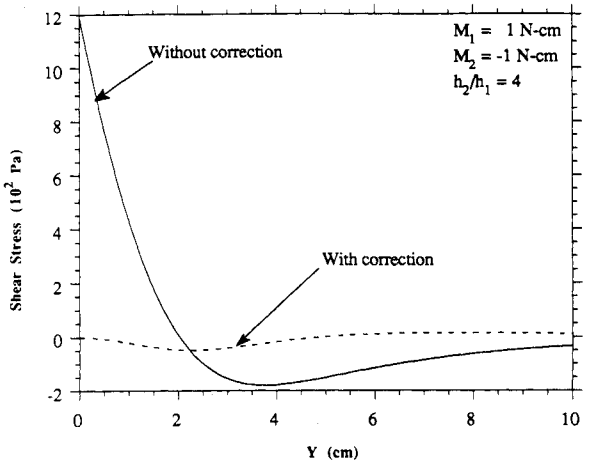

Fig. 5 Shear stress distribution on face A′B′ with and without correction.

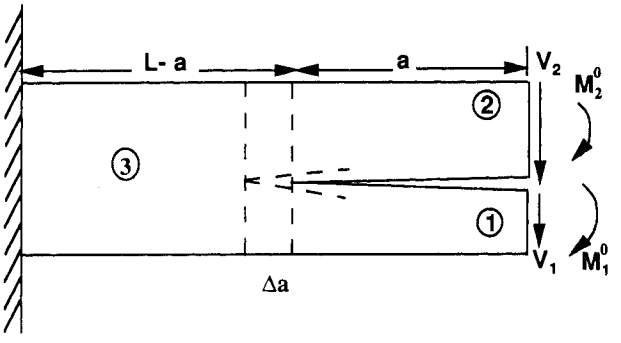

Fig. 6 Strain-energy variation due to crack extension.

on planes AB and A′B′, respectively. It is evident that, with the antimoment correction, the shear stress is negligibly small as compared with that without the correction.

Strain-Energy Release Rate

The strain-energy release rate for the cracked beam can be calculated using Eq. (1). Alternatively, it can be evaluated by the strain-energy increment ΔU associated with a crack extension Δa. Referring to Fig. 6, it is easy to see that, without the consideration of joint flexibility at the crack tip,

$$\Delta U = \Delta U_1 + \Delta U_2 - \Delta U_3 \quad (15)$$

where

$$\Delta U_1 = \left(\frac{M_1^2}{2EI_1} + \frac{V_1^2}{2\kappa GA_1}\right)\Delta a$$

$$\Delta U_2 = \left(\frac{M_2^2}{2EI_2} + \frac{V_2^2}{2\kappa GA_2}\right)\Delta a \quad (16)$$

$$\Delta U_3 = \left[\frac{(M_1+M_2)^2}{2EI_3} + \frac{(V_1+V_2)^2}{2\kappa GA_3}\right]\Delta a$$

where $I_i (i = 1, 2, 3)$ and $A_i (i = 1, 2, 3)$ are the moments of inertia and cross-sectional areas of the three beam segments. Note that the transverse shear deformation is included. In this study the shear correction coefficient is $\kappa = \pi^2/12$, as suggested by Mindlin.[15]

If the root rotations of the beams are considered, then additional strain-energy increment ΔU_{end} must be added. This amount of energy increment results from the change of root moments M_1 and M_2 due to crack extension Δa. We have

$$M_1(a + \Delta a) = M_1(a) + V_1\Delta a \quad (17)$$

$$M_2(a + \Delta a) = M_2(a) + V_2 \Delta a \tag{18}$$

The strain-energy increment at the joint due to the crack extension is given by

$$\Delta U_{\text{end}} = \tfrac{1}{2}M_1(a + \Delta a)\,\theta_1'(a + \Delta a) - \tfrac{1}{2}M_1(a)\theta_1'(a) + \tfrac{1}{2}M_2(a + \Delta a)\theta_2'(a + \Delta a) - \tfrac{1}{2}M_2(a)\theta_2'(a) \tag{19}$$

Substituting Eq. (14) together with Eqs. (17) and (18) into Eq. (19), we obtain

$$\Delta U_{\text{end}} = \left[M_1 V_1 (S_{11} - S_0) + (M_2 V_1 + M_1 V_2) \times \left(\frac{S_{21} + S_{12}}{2} - S_0 \right) + M_2 V_2 (S_{22} - S_0) \right] \Delta a \tag{20}$$

In deriving the previous equation, the quadratic terms in Δa have been neglected.

From Eq. (20), we note that $\Delta U_{\text{end}} = 0$ if the applied load consists of only moments but no shear forces.

The strain-energy release rates for the beam (with a rigid joint) and modified beam (with a flexible joint) models are obtained as

$$G_b = \frac{\Delta U}{\Delta a} \tag{21}$$

and

$$G_m = \frac{\Delta U + \Delta U_{\text{end}}}{\Delta a} \tag{22}$$

respectively.

Table 1 Comparison for adequacy of modified beam model with various other models for predicting strain-energy release rate (10^{-3} N-cm^2/cm) under shear loading ($h_1 = 1$ cm, $V_1 = 6$ N)

h_2/h_1	a/h_1	V_2/V_1	G_b	G_m	G_f	G_{sp}	G_K
1	5	−1	1.559	1.952	1.986	1.888	1.993
1	5	1	1.157	1.260	1.256	1.200	1.483
1	10	−1	6.188	6.973	7.029	6.840	7.029
1	10	1	4.629	4.834	4.824	4.680	5.260
4	10	−1	3.144	3.531	3.571	3.405	3.571 5.017
4	10	1	3.039	3.327	3.369	3.210	3.453 5.200

Table 2 Comparison for adequacy of modified beam model for predicting mode I strain-energy release rate (10^{-4} N-cm^2/cm) under shear loading ($h_1 = 1$ cm, $h_2/h_1 = 1$; $V_1 = 6$ N, $V_2/V_1 = -1$)

a/h_1	G_b	G_m	G_f	$(G_f - G_m/G_f) \times 100$
3	5.717	8.073	8.326	3.04
5	15.591	19.518	19.861	1.73
7	30.403	35.901	36.333	1.19
9	50.151	57.220	57.739	0.90
11	74.837	83.477	84.079	0.72
13	104.460	114.670	115.350	0.59
15	139.020	150.802	151.550	0.49

Table 3 Comparison for adequacy of modified beam model for predicting mode II strain-energy release rate (10^{-4} N-cm^2/cm) under shear loading ($h_1 = 1$ cm, $h_2/h_1 = 1$; $V_1 = 6$ N, $V_2/V_1 = 1$)

a/h_1	G_b	G_m	G_f	$(G_f - G_m/G_f) \times 100$
3	4.166	4.781	4.768	−0.27
5	11.571	12.598	12.561	−0.29
7	22.680	24.117	24.056	−0.25
9	37.191	39.339	39.252	−0.22
11	56.006	58.263	58.147	−0.20
13	78.223	80.891	80.739	−0.19
15	104.143	107.221	107.030	−0.18

Fig. 7 Typical finite element mesh used for two-dimensional analysis.

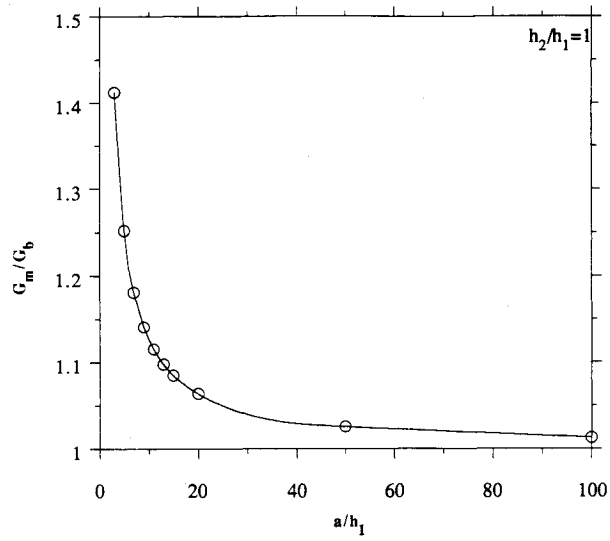

Fig. 8 Comparison of strain-energy release rate predicted by modified and classical beam theories at various crack lengths for mode I fracture (circle—analytical, solid line—cubic spline fit).

Evaluation of Beam Models

To evaluate the accuracy of the beam models, we used the finite element method to calculate the strain-energy release rate for cracked beams of different split beam thickness ratios (h_2/h_1) subjected to different loads. The ABAQUS finite element code was used to perform these analyses with the eight-node isoparametric plane-stress element. A typical finite element mesh for a symmetrically split beam is shown in Fig. 7. The model has 3841 nodes, 1200 elements, and 7682 degrees of freedom. All of the shear loads applied were considered to be uniformly distributed. The strain-energy release rates were evaluated using the J-integral.

The material constants used in the analysis are $E = 70$ GPa and $\nu = 0.3$. The dimensions of the cracked beam are given by $h_1 = 1$ cm with h_2/h_1 and a/h_1 varying. The strain-energy release rate is given in terms of N-cm/cm^2.

Table 1 lists the strain-energy release rates for a cracked beam under shear force loading calculated using the finite elements G_f, the Timoshenko beam model with a rigid joint G_b, the present modified Timoshenko beam model with a flexible joint G_m, the split beam model G_{sp} by Sankar and Hu[13] and the elastic foundation model G_K by Kanninen[10,11] and Williams.[12] In Sankar and Hu's split beam model, the axial and transverse springs are assumed rigid, and the rotational spring is taken to have vanishing rigidity. By so doing, the issue concerning the values of the spring constants is avoided. In the Kanninen-Williams approach, the spring constant is not uniquely defined if $h_1 \neq h_2$. In Table 1, both h_1 and h_2 are used to obtain the spring constant from Eqs. (2) and (3). The first value of G_K corresponds to the use of h_1, and the second value of G_K corresponds to the use of h_2. The value of χ is taken as 0.66.

From the comparison presented in Table 1, it is evident that the present modified beam model yields consistently better results than other beam models, especially for small cracks.

Tables 2 and 3 present the results for mode I and mode II cases with varying crack lengths in a split beam of equal thicknesses ($h_2/h_1 = 1$). The results show very good agreement between the finite element and modified beam predictions. Contrary to the general notion, the error of the beam model

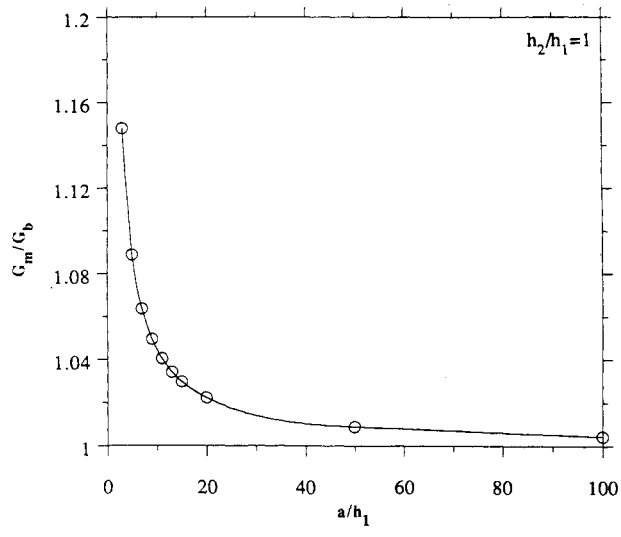

Fig. 9 Comparison of strain-energy release rate predicted by modified and classical beam theories at various crack lengths for mode II fracture (circle—analytical, solid line—cubic spline fit).

with a rigid joint is not very small for crack lengths to thickness ratio up to 15. To assess the range of validity of the beam model with rigid joint with respect to crack length, we extended the results of Tables 2 and 3 to include larger crack lengths. Since G_m and G_f agree very well, only G_b and G_m are calculated for larger values of a/h_1. The results are plotted in Figs. 8 and 9. It can be concluded that even for very large cracks (relative to beam thickness) the effect of joint flexibility may not be negligible.

Table 4 compares the three models (G_b, G_m, and G_f) under the action of pure moments. It is found that, within the limit of numerical errors, all three models predict the same value for the energy release rate. This outcome should have been expected from Eq. (20) for ΔU_{end}. For pure moment loading, the strain energy in the flexible joint remains constant as the crack extends. As a result, $\Delta U_{\text{end}} = 0$, and no modification on the strain-energy release rate is necessary. Thus, for pure moment loading, the beam model with rigid joint yields excellent results.

Table 5 shows the accuracy of the modified beam model for the symmetrically split beam under the action of different types of transverse loads. For the same crack length, the maximum difference between the finite element and the modified beam model is found for pure mode I and minimum for pure mode II. All other combinations of loadings are expected to fall within these two limits for the same crack length.

Table 6 lists the results for an unsymmetrically split beam ($h_2/h_1 = 4$) under unsymmetrical loadings for $a/h_1 = 20$. Again, the modified beam model gives excellent agreement with the finite element solutions.

The joint flexibility given by Eq. (14) is derived with the aid of antimoments in a half-plane problem to approximately satisfy the shear stress free condition on the surfaces of the uncracked portion of the beam. In the case of an unsymmetrically split beam with $h_2/h_1 > 13$, it is found that $S_{22} - S_0$ would become negative. This indicates that $\theta_2 \approx \theta_3$ for $h_2/h_1 > 13$ and $\theta_1 \approx \theta_3$ for $h_1/h_2 > 13$. Thus, the joint flexibility can be approximated by

$$\theta_1' = (S_{11} - S_0)M_1 \qquad \text{for} \qquad h_2/h_1 > 13 \tag{23}$$

and

$$\theta_2' = (S_{22} - S_0)M_2 \qquad \text{for} \qquad h_1/h_2 > 13 \tag{24}$$

Mode Partitioning

For fracture analysis, it is of interest to separate the strain-energy release rate into two parts corresponding to modes I and II, respectively. The separation can be performed if the loading can be separated into "symmetric" and "antisymmetric" loadings such that, in the crack plane ahead of the crack tip, shear stress and transverse normal stress, respectively, vanish. For a symmetrically cracked beam ($h_2/h_1 = 1$), this load separation can easily be accomplished. However, for unsymmetrically cracked beams ($h_1 \neq h_2$), the unsymmetric geometry makes the intended load separation impossible. Williams[6] incorrectly proposed the following mode partitioning formulas:

$$M_1 = M_{\text{II}} - M_{\text{I}} \tag{25}$$

$$M_2 = \psi M_{\text{II}} + M_{\text{I}} \tag{26}$$

where M_{I} and M_{II} correspond to mode I and mode II loadings, respectively, and

$$\psi = \left(\frac{1-\xi}{\xi}\right)^3$$

$$\xi = \frac{h_1}{h_1 + h_2}$$

The derivation was based on the assumption that under mode II action the curvatures of the two beams at the crack tip must be equal, i.e.,

$$\frac{M_{\text{II}}}{EI_1} = \frac{\psi M_{\text{II}}}{EI_2} \tag{27}$$

It can easily be shown that M_1 and M_{II} obtained according to Eqs. (25) and (26) produce symmetric and antisymmetric loadings, respectively, only for the special case $h_1 = h_2$. For unsymmetrically cracked beams, the strain-energy release rates partitioned according to Eqs. (25) and (26) deviate greatly from the two-dimensional finite element solutions.

We also used Sankar and Hu's split beam model to partition mode I and mode II strain-energy release rates using the crack closure method. The mode I strain-energy release G_{I} was taken as the work done in closing the relative transverse displacements of the two split beam segments, and the mode II strain-energy release rate G_{II} was taken as the work done in

Table 4 Comparison for adequacy of modified beam model for predicting strain-energy release rate (10^{-6} N-cm^2/cm) under moment loading ($h_1 = 1$ cm, $h_2/h_1 = 1$; $M_1 = 1$ N-cm, $a/h_1 = 10$)

M_2/M_1	G_b	G_m	G_f	$(G_f - G_m/G_f) \times 100$
−1	1.714	1.714	1.715	0.06
0	0.750	0.750	0.750	0.00

Table 5 Comparison for adequacy of modified beam model for predicting strain-energy release rate (10^{-2} N-cm^2/cm) under various kinds of shear loading ($h_1 = 1$ cm, $h_2/h_1 = 1$, $a/h_1 = 10$; $V_1 = 16$ N)

V_2/V_1	G_b	G_m	G_f	$(G_f - G_m/G_f) \times 100$
0	1.923	2.099	2.107	0.38
−1	4.400	4.959	4.998	0.78
1	3.291	3.437	3.430	−0.20

Table 6 Comparison for adequacy of beam model for predicting strain-energy release rate (10^{-2} N-cm^2/cm) for asymmetrically split beam under various kinds of shear loadings (N) ($h_1 = 1$ cm, $h_2/h_1 = 4$, $a/h_1 = 20$)

Loading	G_b	G_m	G_f	$(G_f - G_m/G_f) \times 100$
$V_1 = 0$, $V_2 = -64$	1.075	1.205	1.188	−1.43
$V_1 = 16$, $V_2 = -64$	10.358	11.239	11.270	0.28
$V_1 = 16$, $V_2 = 0$	8.712	9.184	9.231	0.51
$V_1 = 16$, $V_2 = 64$	9.216	9.539	9.572	0.35

closing the relative axial displacements. We found that the values of G_I and G_{II} depend highly on the finite element size near the crack tip. In fact, a violent oscillatory behavior in G_I and G_{II} appeared as the finite element mesh near the crack tip was refined. This behavior resembles that of the finite element modeling of an interfacial crack between two dissimilar media.[16]

It is felt that, although the total strain-energy release rate for cracked beams can be accurately calculated with beam theories without modeling the near-tip singular stress field, mode partitioning may not be properly done without the use of the near-tip fields.

Conclusions

Based on an approximate two-dimensional elasticity solution, the flexibility of the joint of beam segments in a cracked beam was explicitly derived. In calculating the strain-energy release rate in cracked beams with the Timoshenko beam theory, we used this result to add additional strain-energy release during crack extension. Numerical evaluation of the present modified beam model in calculating the strain-energy release rate was carried out for various cracked beams under various loading conditions. Comparisons with the two-dimensional finite element solutions indicated that the new beam model can accurately predict the strain-energy release rate even for very short crack lengths. It was also shown that the present model is superior to existing methods using beam theory. It has also been demonstrated that the conventional method that assumes a rigid joint yields accurate strain-energy release rates only for very large crack-length-to-beam-thickness ratios or for the case of pure bending moments in the split segments of the beam.

Acknowledgment

Financial support for this work was provided by NASA Langley Research Center under Grant NAG-1-1323 to Purdue University. Technical monitors for this project were Jerry Housner and John Wang.

References

[1]Rice, J. R., "A Path-Independent Integral and the Approximate Analysis of Strain Concentration by Notches and Cracks," *Journal of Applied Mechanics,* Vol. 35, No. 2, 1968, pp. 376–386.

[2]Rybicki, E. F., and Kanninen, M. F., "A Finite Element Calculation of Stress Intensity Factors by a Modified Crack Closure Integral," *Engineering Fracture Mechanics,* Vol. 9, No. 4, 1977, pp. 931–938.

[3]Jih, C. J., and Sun, C. T., "Evaluation of a Finite Element Based Crack-Closure Method for Calculating Static and Dynamic Strain Energy Release Rates," *Engineering Fracture Mechanics,* Vol. 37, No. 2, 1990, pp. 313–322.

[4]Kanninen, M. F., and Popelar, C. H., *Advanced Fracture Mechanics,* Oxford Univ. Press, New York, 1985.

[5]Pook, L. P., "Approximate Stress Intensity Factors Obtained from Simple Plate Bending Theory," *Engineering Fracture Mechanics,* Vol. 12, No. 4, 1979, pp. 505–522.

[6]Williams, J. G., "On the Calculation of Energy Release Rates for Cracked Laminates," *International Journal of Fracture,* Vol. 36, 1988, pp. 101–119.

[7]Nilsson, K.-F., and Storakers, B., "On Interface Crack Growth in Composite Plates," *Journal of Applied Mechanics,* Vol. 59, 1992, pp. 530–538.

[8]Yin, W.-L., and Wang, J. T. S., "The Energy-Release Rate in the Growth of a One-Dimensional Delamination," *ASME Journal of Applied Mechanics,* Vol. 51, 1984, pp. 939–941.

[9]Farris, T. N., and Doyle, J. F., "A Global/Local Approach to Lengthwise Cracked Beams: Static Analysis," *International Journal of Fracture,* Vol. 50, 1991, pp. 131–141.

[10]Kanninen, M. F., "An Augmented Double Cantilever Beam Model for Studying Crack Propagation and Arrest," *International Journal of Fracture,* Vol. 9, 1973, pp. 83–92.

[11]Kanninen, M. F., "A Dynamic Analysis of Unstable Crack Propagation and Arrest in the DCB Test Specimen," *International Journal of Fracture Mechanics,* Vol. 10, 1974, pp. 415–430.

[12]Williams, J. G., "End Corrections for Orthotropic DCB Specimens," *Composite Science and Technology,* Vol. 35, 1989, pp. 367–376.

[13]Sankar, B. V., and Hu, S., "Dynamic Delamination Propagation in Composite Beams," *Journal of Composite Materials,* Vol. 25, No. 11, 1991, pp. 1414–1426.

[14]Timoshenko, S. P., and Goodier, J. N., *Theory of Elasticity,* McGraw-Hill, New York, 1987.

[15]Mindlin, R. D., "Influence of Rotatory Inertia and Shear on Flexural Motion of Isotropic, Elastic Plates," *Journal of Applied Mechanics,* Vol. 18, No. 1, 1951, pp. 31–38.

[16]Sun, C. T., and Jih, C. J., "On Strain Energy Release Rates for Interfacial Cracks in Bi-Material Media," *Engineering Fracture Mechanics,* Vol. 28, No. 1, 1987, pp. 13–20.